Towards a User-wheelchair Shared Control Paradigm for Individuals with Severe Motor Impairments

Alfredo Chávez Plascencia and Jaroslav Rozman
Faculty of Information Technology, IT4Innovations Centre of Excellence, Brno University of Technology, Božetěchova 1/2 612 66, Brno, Czech Republic

Keywords: Assistive Technology, Sensor Fusion, Autonomous Wheelchair.

Abstract: This paper presents a work in progress study of a novel user-wheelchair shared control paradigm for individuals with severe motor impairments, which consists of an optimal distribution between several modes, from full user control up to autonomous driving one. To this end, a C400 Permobil wheelchair has been equipped with a control command communication interface and with a scanning laser and a RGB-D sensors to carry out the automation algorithms that are part of the robot operating system (ROS) framework. Moreover, sensor data fusion for map making based on the Bayesian method is applied to the Xtion Pro Live RGB-D camera and the Hokuyo laser sensor data readings. These latter are interpreted by a probabilistic heuristic model that abstracts the beam into a ray casting to an occupied grid cell. Preliminary pilot tests were performed in two different room shapes. The first one in a two room laboratory with a narrow doorway, and the second one in a corridor. The former experiment was dropped due to failure to success, whereas, the latter was a successful one. This has been tested with three different modalities; hand-joystick, tongue-joystick and autonomous modes respectively. The successful results of the second pilot-test have proven the feasibility of using a combination of autonomous and manual control of a powered wheelchair in order to continue development towards a shared-control paradigm.

1 INTRODUCTION

Powered wheelchairs (PWC) are used to assist mobility of individuals with severe motor disabilities, such as those with tetraplegia. Users that still maintain some degree of motor control of arms or hands use a joystick in order to control the direction and speed of the PWC. On the other hand, users with more severe or complete motor disabilities have to rely on alternative control interfaces that can detect head movement (Christensen and Garcia, 2003), chin movement (Cooper et al., 2002), gaze (San Agustin et al., 2009), tongue movement (Xueliang and Maysam, 2010) (Lund et al., 2010) and even forehead muscular activity and brain waves (Torsten, Felzer and Rainer, Nordman, 2007). Thus, research has been done to develop devices that can interface the remaining functional parts of such individuals. Many of these interfaces require the user to sustain high levels of concentration for navigating in environments with many obstacles. Some systems might be tedious and tiresome to use, especially when constantly maneuvering a wheelchair, while others might interfere with the normal use of the user's vision or head, eyes or tongue movement. Allowing certain degree of autonomy to the wheelchair might relieve the users of the burden of long periods of concentration or fatigue, and allow a more free use of their own eyes, tongue or head movement while driving the wheelchair. However, a fully autonomous system is not desired, since the users should be allowed as much control of the wheelchair as their capabilities and degree of disability allows them to have, and without compromising the use of their vision, speech head movement unnecessarily or for prolonged periods of time.

Some related research work has been focused on sharing the wheelchair control with the user. For instance, a shared wheelchair control method for obstacle avoidance is presented in (Petry et al., 2010). This method mainly proposes using potential field for path planning and shares the wheelchair control to help the user to avoid obstacles. (Faria et al., 2013) presents a manual-shared-automatic method for controlling a PWC. The automatic control consists of following points without human intervention, the shared control acts in safety situations, mainly when there

Plascencia, A. and Rozman, J.
Towards a User-wheelchair Shared Control Paradigm for Individuals with Severe Motor Impairments.
DOI: 10.5220/0005973302460253
In *Proceedings of the 13th International Conference on Informatics in Control, Automation and Robotics (ICINCO 2016) - Volume 2*, pages 246-253
ISBN: 978-989-758-198-4

is a potential collision. (Jiding et al., 2014) presents a shared-control wheelchair based on Brain Computer Interface (BCI), where the shared-control provides assistance strategy to control the wheelchair when it is in a collision region.

Based on the present research our main goal is to investigate further in order to find the optimal distribution of control tasks between the user and the intelligent wheelchair controller. This shall help to develop a novel user-wheelchair shared control paradigm that takes into consideration the needs and abilities of individuals with severe motor impairments, and allows them to control a PWC from a user-controlled, through a semi-autonomous up to a fully autonomous way. The amount of autonomy in the semi-autonomous control mode, also referred to as "shared-control", should depend on the user preferences, the degree of disability of the user and the amount of input the user can give in a fast and efficient way, allowing the user and the wheelchair to "share" control tasks.

For this study, two different environment shapes were taken into account in order to validate the preliminary paradigm. The first shape is a two room laboratory and the second one is a corridor. The experiments of the first shape were dropped early due to failure to success and are not presented in this article. Instead an analysis on how to overcome them is presented in the conclusion. On the other hand, the second pilot tests were successful and are presented in this work.

From the alternative control interfaces for a PWC, we have chosen to use a tongue-controlled interface. Using the tongue to control a PWC seems to be a promising alternative for the following reasons. Firstly, the tongue is able to perform sophisticated motor control and manipulation tasks with many degrees of freedom. Secondly, it is able to move rapidly and accurately and does not fatigue easily and can be controlled naturally without requiring too much concentration. Georgia Institute of Technology has developed a tongue drive system (TDS) that consists of a headset and a magnetic tongue barbell. Through a smartphone (iPhone), the TDS is able to interpret five tongue movement commands: forward (FD), backward (BD), turning right (TR), left (TL) and stopping (N) (Jeonghee et al., 2008), (Xueliang and Maysam, 2010), (Andreasen, 2006),(Jeonghee et al., 2012). Similarly, an intra-oral inductive tongue control system (ITCS) has been designed and built at Aalborg University. It interpolates the sensor signals to emulate an intra-oral touchpad that can proportionally control the direction and speed of the PWC (Caltenco et al., 2011).

Figure 1: The C400 permobil wheelchair equipped with a control command communication interface and with a scanning laser and a RGB-D sensors.

2 SYSTEM DESCRIPTION

2.1 Communication Interface

The C400 Permobil PWC as shown in Figue 1 comes with an Easy Rider wheelchair interface, from HMC International, an Easy Rider display unit and a joystick. The standard joystick mode accepts as input signals a reference value of 5V and two analog voltage values in the range of 4V to 6V to proportionally move the PWC from right to left and from back to forward. To this end, an interface to send velocity control commands (VCC) from the computer to the motors has been developed using an Arduino UNO board. The Arduino board receives two VCC bytes (one for left-right and one for forward-backward directions) and generates two pulse width modulated (PWM) signals in the range of 0 to 5V. The signals are converted to analog voltage using a simple RC low-pass filter and stepped-up using a single supply non-inverting DC Summing Amplifier. The resulting voltage is used to emulate the analog joystick position as an input to the Easy Rider interface. The Easy Rider interface then sends the necessary control signals to the wheelchair's motor controller.

2.2 Alternative Control Interface

The ITCS (Caltenco et al., 2011), consists of two separate parts, the intra-oral device and an external con-

troller. The intra-oral device detects tongue movements and wirelessly transmit signals to the external controller, which connects to the Easy Rider interface via the Joystick Input and to the computer via bluetooth. The ITCS's external controller interprets and process tongue movement signals and transforms them into joystick or mouse commands that can be sent to the wheelchair or the computer. The computer is a Lenovo T540p with an Intel(R) Core(TM) i5-4200M CPU @ 2.50GHz running Ubuntu 12.04 (precise), The system previously explained can be depicted in Figure 2.

2.3 Sensors

Data from the environment is obtained by a Hokuyo UTM-30LX scanning laser range finder. It has a sensing range from 0.1m to 30m. Measurement accuracy is within 3mm tolerance up to 10m of the sensor's range. The scanning rate is 25 milliseconds across a 270 range.

The Asus Live Xtion Pro RGB-D camera, popular in various robotic projects. It has a field of view of 58° $H, 45^\circ$ V (Horizontal, Vertical). Meanwhile, the sensor's depth image size is 640×480 pixels with a total of $307,200$ pixels. The distance of use of the sensor is between $0.8m$ and $3.5m$.

3 SENSOR FUSION AND MODELS

The laser can measure the distance to an object quite accurately. However, there is an uncertainty in the pulse that is reflected back to the sensor. On the other hand, the RGB-D sensor also returns the depth to each pixel, which uncertainty also need to be modeled. The approach taken by (Moravec and Elfes, 1985), (Elfes, 1989b) and (Stěpán et al., 2005) to model the occupied and empty regions of the sonar beam can be taken into consideration to model the uncertainty in both sensors data readings.

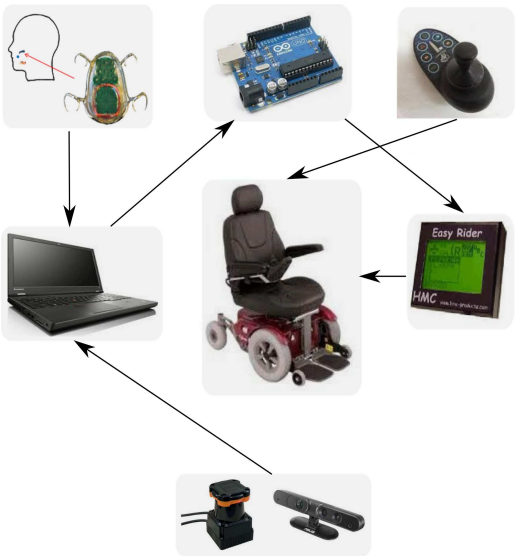

Figure 2: Overview of the System.

RGB-D and laser probabilistic sensor data fusion is proposed to complement both sensors field of view, (Chávez and Karstoft, 2014). Thus, Elfes (Elfes, 1989a) has proposed in his previous work the use of a recursive Bayes formula to update the occupancy grid for multiple sensor observations.

4 SOFTWARE ARCHITECTURE

Robot operating system (ROS) (Quigley et al., 2009) is proposed as the software architecture to achieve the different modes the user can select to drive the PWC. The navigation stack (NS), which is a set of configurable nodes, has been configured properly to the shape and dynamics of the PWC to be performed at a high level. Broadly speaking, the heart of the navigation stack is the move base node which provides a high level interface between odometer, PWC base controller, sensors, sensor transforms, map server and monte carlo localization algorithm (AMCL) nodes to the local and global planners.

5 METHODS

One participant with no previous experience driving a PWC participated in this pilot study. To this end, a $5 \times 2 \times 2$ factorial experiment has been designed with the following factors (independent variables):

1. Control mode [M] with five levels:
   - M_A (autonomous-mode)
   - M_{JG} (user-mode using a usb gamepad joystick)
   - M_{JW} (user-mode using wheelchair's joystick)
   - M_{JT} (user-mode using tongue-joystick)
2. Wheelchair velocity [V] with two levels:
   - V_L (low velocity, 0.186 $\frac{m}{sec}$)
   - V_H (high velocity, 0.243 $\frac{m}{sec}$)
3. Number of obstacles [O] with two levels:
   - O_F (few obstacles on the path, 5 obstacles)
   - O_P (plenty obstacles on the path, 10 obstacles)

Moreover, the following dependent variables are used to compare performance of each test scenario:

1. T_P (path's completion time)
2. V_A (average velocity)
3. N_C (number of collisions)
4. d_p (path's distance).

The experiment design is three-dimensional in the within subject variables. However, it is not fully factorial, since the tongue-joystick control mode (M_{JT}) did not perform the experiment using different velocity conditions [V], giving a total of 18 within subject conditions, instead of 20.

A graphical user interface (GUI) has been implemented, where three modes can be selected by the operator.

- Joystick mode (M_J), the PWC is able to be manipulated by the commands emulated from the control level, e.g. forward (F), backward (B), right (R), left (L) and stopping (S). This can be done using any of the three control interfaces (wheelchair joystick (M_{JW}), gamepad joystick (M_{JG})or tongue joystick (M_{JT})).
- Semi-autonomous mode (M_S), The process is comprise of the following steps; 1.- Real obstacles have been placed in the environment. 2.- A global map with no obstacles is used. 3.- Joystick mode is applied in order for the user to rotate the PWC left or right while trying to find a suitable path. And, once this path has been spotted the user can select the (F) joystick command. 3.- Then, a shared-control algorithm is activated that finds a suitable goal in the desired direction at the end of the map. 4.- Afterwrads, the NS uses this goal to move the PWC towards that direction avoiding obstacles on its way till either the user cancel the action or the PWC reaches the goal coordinates.
- Autonomous mode (M_A), the user selects the coordinates of a destination point on a map of the known environment using the ITCS. The user can always be able to override autonomous control and take control of the wheelchair at any moment.

The C400 Permobil wheelchair serves as experimental testbed. The tests were carried out with real data in an indoor laboratory environment. To this end, the map of the indoor environment was built prior to the tests, this was achieved by using the fused Hokuyo laser and RGB-D data, which have been placed in front of the PWC.

The RGB-D catches 3D depth data that is projected into 2D to ease the integration process. At the same time, the laser field of view also catches 2D depth data. Furthermore, sensor registration is used to align both sensor readings, so they can not suffer from misalignment that can potentially cause errors

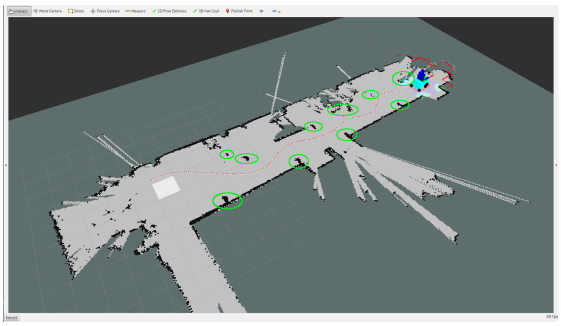

Figure 3: Schematics of the map.

in the fused grid maps. In each measurement the laser scans a total of 512 readings distributed along 180^0 . Meanwhile, the ROS depthimage_to_laserscan package is used to project RGB-D readings into 2D. Then, each sensor reading is interpreted by the heuristic sensor model. Afterwards, the recursive Bayes formula is applied to fuse and update the data in each probabilistic grid map, e.g. the RGB-D and laser maps.

To visualize the map making process and the navigation, Figure 3 shows the RVIZ which is a ROS visualization tool. In the right part, the PWC-URDF (unified robot description format) model can be seen, the local map is represented as inflated sky-blue obstacles that surround the URDF. The obstacles in the global map are represented as black and the location of the main obstacles are surrounded by a green ellipse, while the light and dark grays represents the empty and unknown areas respectively, the fused sensor readings that are used for localization, navigation and to feed the local map can be spotted as red contour that are situated in front of the PWC. And, the path travel can also be seen on the empty area of the map.

6 MAIN FINDINGS AND RESULTS

Figures 4, 6 and 8 show the bar plots of the pilot tests dependent variables T_P, V_A, N_C and d_P outcomes for the factors ([M], [V], [O]) and their corresponding levels (M_A,M_S,M_{JG},M_{JW},M_{JT}), (V_L,V_H) and (O_F,O_P).

It can be observed in Figure 4 that (O_P, V_H, M_A) and (O_P, V_L, M_A) takes almost the same time to travel the path even though the velocities are different. Whereas, (O_F, V_H, M_A) and (O_F, V_L, M_A) takes different time due to the reduction of obstacles. Then, when driving the PWC in M_S, (O_F, V_L) takes less time than (O_P, V_L), in the same way (O_P, V_L) takes more time than (O_P, V_H). It can also be observed that (O_p, M_{JT}) is the longest path's time of all modes.

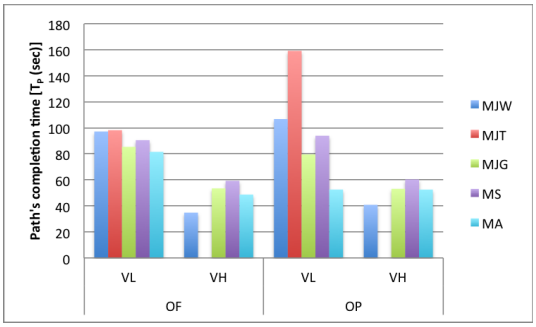

Figure 4: Time of the path.

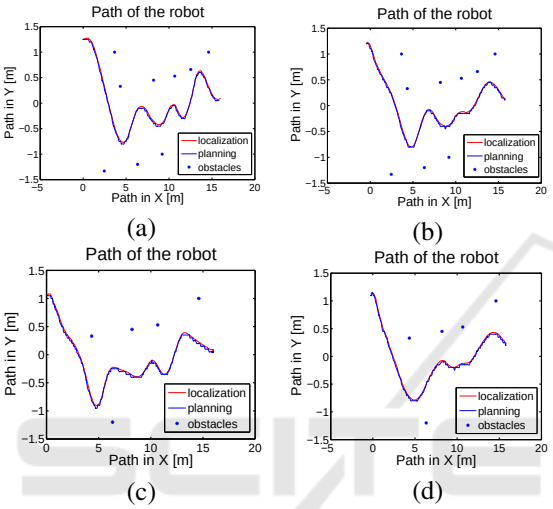

Figure 5: Autonomous mode (M_A); a) fast velocity with many obstacles. b) slow velocity with many obstacles c) slow velocity with few obstacles. d) fast velocity with few obstacles.

This fact could be because the user was inexperienced with the ITCS. And, it is believed that this situation can be improved by practicing using the tongue to control the wheelchair. In the other hand $(O_p,\ M_{JT})$ takes less time, this is due to the fact that there is less obstacles and the user is able to control better the ITCS. However, the shortest path's time of all modes is $(O_F,\ V_H,\ M_{JW})$. It is important to mention that user was proficient and has experience in controlling hand-operated joysticks like the (M_{JW}).

Figure 5 shows the M_A plots of the path traveled by the PWC for the different velocities and and also shows the location of the obstacles. The blue path correspond to the global planner whereas the red paths correspond to the position of the PWC based on the localization algorithm. The planner is computing new paths constantly from its current position to the goal while the PWC is traveling, producing a different final path when compared with the initial one. In this context the PWC is able to follows constantly and quite accurately the re-planned paths, hence the final path.

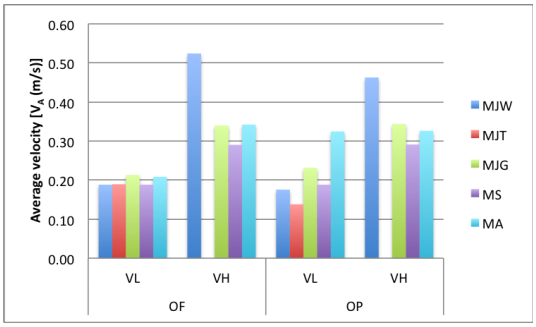

Figure 6: Average velocity.

Figure 6 depicts the results of the V_A pilot test. It can be seen that the average velocity between $(O_P,\ V_L,\ M_A)$ and $(O_P,\ V_H,\ M_A)$ is almost the same even though the PWC was run in two different velocities. The reason for this could be that while driving in $(V_H,\ M_A)$, there is a delay for the PWC to react to follow the initial path allowing the global planner to constantly computing paths a bit longer than it should be. The situation changes in M_A when there is O_F, this means that the planner computes a path with less pronounced curves, making the PWC to follow closer the constantly computed paths. In the other hand, $(O_P,\ V_L,\ M_S)$ takes slower velocity when compared with $(O_P,\ V_H,\ M_S)$. The fact for this could be that the initial point was in the right side bottom of the map, allowing the planner to plan a more straight path, so the PWC did not face sharp curves as in the later case. Moreover, $(O_p,\ M_{JT})$ and $(O_F,\ V_H,\ M_{JW})$ show the slowest and fastest traveled paths of all modes respectively.

Figure 7 shows the plots of the path travel by the PWC in its independent variables, as in the M_S mode the path traveled by the PWC follow quite accurately the path planned by the global planner.

The collision outcome corresponding to the dependent variable N_C is depicted in Figure 8. It can be noticed that the PWC touches obstacles just in M_S, one in $(O_p,\ V_H)$, two in $(O_p,\ V_L)$ and one $(O_F,\ V_H)$ respectively.

Figure 9 shows the path for the USB gamepad joystick mode M_{JG} for different velocities (V_H, V_L) and for different obstacles $(O_P\ O_F)$.

Figure 10 depicts the path travel distance d_P outcome, it clearly shows the longest distance is $(O_P,\ V_L,\ M_{JT})$ as well as the shortest one (O_F, V_H, M_A).

Figure 11 shows the path for the PWC joystick mode M_{JW} for different velocities (V_H, V_L) and for different obstacles $(O_P\ O_F)$.

Figure 12 and 13 show the the mean and variance of the planned paths and the executed ones in M_A and M_S respectively. Whereas Figure 14 depicts

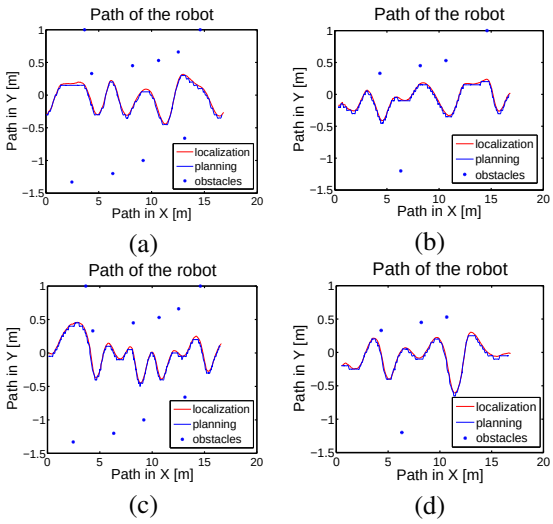

Figure 7: Semi-autonomous mode (M_S); a) fast velocity with many obstacles. b) slow velocity with many obstacles c) slow velocity with few obstacles. d) fast velocity with few obstacles.

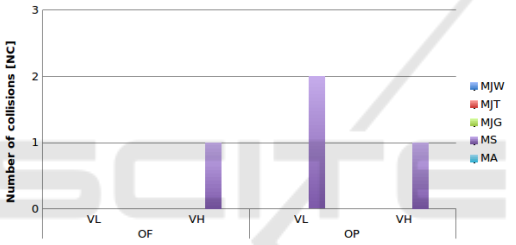

Figure 8: Collisions.

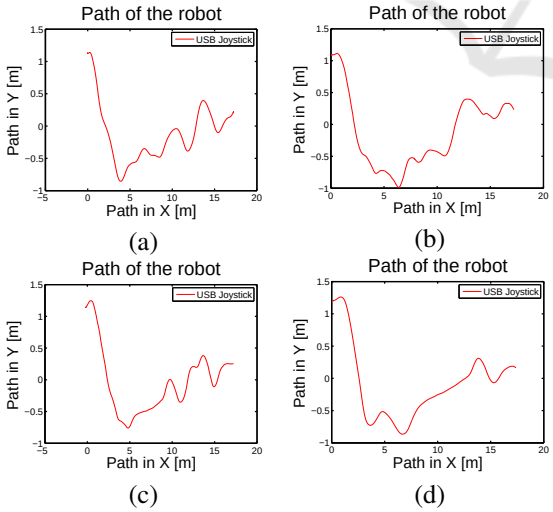

Figure 9: USB gamepad joystick mode (M_{JG}); a) fast velocity with many obstacles. b) slow velocity with many obstacles c) slow velocity with few obstacles. d) fast velocity with few obstacles.

the tongue joystick mode (M_{JT}) with many and few obstacles.

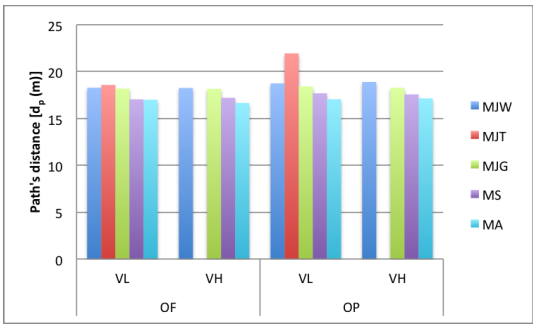

Figure 10: Distance of the path.

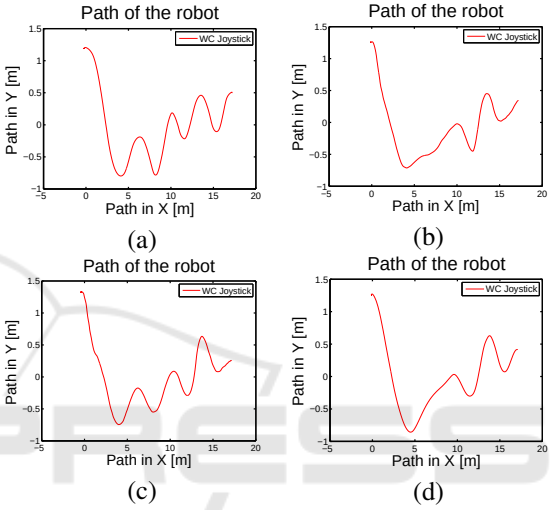

Figure 11: PWC joystick mode (M_{JW}); a) fast velocity with many obstacles. b) slow velocity with many obstacles c) slow velocity with few obstacles. d) fast velocity with few obstacles.

Figure 12: Mean.

When comparing M_A and M_S in Figure 4 for different obstacles and time paths' travel, one can observe that M_S completes all the paths in a slightly longer time span than M_A. This fact can also be reflected in Figure 6 where V_A in M_S is slower than M_A. The reason for this situation is that in M_S mode, a global map with no obstacles has been used to find a suitable goal in the desired direction which makes

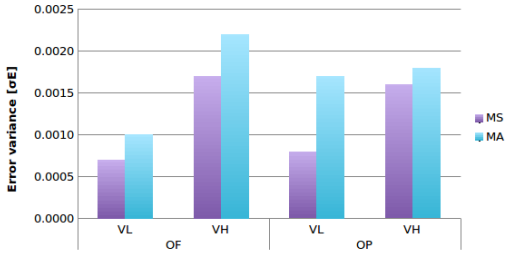

Figure 13: Variance.

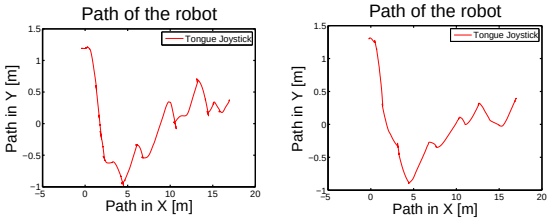

(a) (b)

Figure 14: Tongue joystick mode (M_{JT}); a) many obstacles. b) few obstacles.

the planned path not taking into account the obstacles. Then, the NS relies only in the DWAP to avoid obstacles towards the goal making the new re-calculated paths with more pronounced curves and by consequence longer paths. However, according to Figure 8, M_S touches more obstacles than M_A, this situation could be because in M_S the PWC seeks to go to the end of the map avoiding obstacles on the way and not taking into account the obstacles for the initial path planning as it is done in M_A. According to these two modes, if one wants to go faster and care for not touching obstacles, the M_A is a good choice. When taking an observation to M_J in their three control interfaces M_{JG}, M_{JW} and M_{JT}, Figure 6 shows that the fastest mode is M_{JW} and this is due to the PWC runs without any computer interface and uses all the motors' power, in the other hand the other two modes runs with a computer interface making them slower.

7 CONCLUSIONS

In this described preliminary study, two environment setups were used for the pilot tests; a two room laboratory and a corridor shape. The successful results of the second pilot tests in their independent variables have established the basis for:

- Preparing the framework for a full factorial design. For that, there is a necessity to overcome the issues experienced in the experiments. A similar problem experienced in both experiments is that the planner plans the path too close to the obstacles, especially when it goes through a narrow doorway or turning around a wall corner. In the case of the first experiment the wheelchair could not go through a doorway because a ROS security plugin canceled the navigation. The solution to this problem is to develop two ROS plugins; the first one for global voronoi path planning (Garrido et al., 2006), and the second for escape-security conditions. In the second experiment the PWC touched some obstacles, especially in M_S. The solution to this is to improve the shared-control algorithm, e.g. by taking into account the map with obstacles when calculating the path to the desired direction.
- Testing the system with higher speed. We have tried to push the navigation to its limits and over its limits with the actual high velocity with no success. However, we believe that the main reason is that the performance of the system was not optimal. Therefore, an optimal relation between path-following and high-speed must be found in order to test the system at higher speed.
- Testing the system in all the independent variables under challenged conditions, e.g. paths where the PWC must go through narrow doorways from one room to another, in cluttered spaces and, also with dynamic obstacles.
- Making a proper ANOVA analysis using at least 5 participants per control-mode and several repetitions per experimental condition. Randomization will be necessary.

The actual shared-control strategies have mainly focused on sharing the control of the PWC to the user in collision situations. On the other hand, this study has shown a preliminary optimal distribution of tasks and has provided the basis for further research on optimal distribution of high-level control tasks between the autonomous and the user-controlled modes for different situations depending on the control interface and the users' abilities. We believe that this research will lead to the development of a novel shared-control paradigm for individuals with severe motor impairments. The capabilities of the shared control algorithms need to be tested in indoor environments. The abilities and needs of users with high level spinal cord injury are different from those of spastic users, or users with ALS (Simpson et al., 2008). Therefore, the amount of user-control and the amount of automation required is different for each user and each situation. This not only depends on the amount and quality of input the user can give to the system, but also on the context and the environment that the system is operating in. Therefore, we also believe that when this new

paradigm is fully implemented it will help wheelchair users with severe motor impairments to interact more efficiently with the environment.

ACKNOWLEDGMENT

This work was supported by The Ministry of Education, Youth and Sports from the National Programme of Sustainability (NPU II) project "IT4Innovations excellence in science - LQ1602 and by the project IGA FIT-S-14-2486. It was also performed in collaboration between Brno University of Technology, Czech Republic and Héctor Caltenco who is with the Department of Design Sciences, Certec, Lund University, Sweden.

REFERENCES

Andreasen, S. L. N. S. (2006). An inductive tongue computer interface for control of computers and assistive devices. *IEEE Transactions on biomedical Engineering*, 53(12):2594–2597.

Caltenco, H. A., Lontis, E. R., and Andreasen, S. L. (2011). Fuzzy Inference System for Analog Joystick Emulation with an Inductive Tongue-Computer Interface. In *15th Nordic-Baltic Conference on Biomedical Engineering and Medical Physics (NBC 2011)*, volume 34, pages 191–194. IEEE, Springer Berlin Heidelberg.

Chávez, P. A. and Karstoft, H. (2014). Map building based on a xtion pro live rgbd and a laser sensors. *Journal of Information Technology & Software Engineering*.

Christensen, H. V. and Garcia, J. C. (2003). Infrared Non-Contact Head Sensor, for Control of Wheelchair Movements. *Assistive Technology: From Virtuality to Reality, A. Pruski and H. Knops (Eds) IOS Press*, pages 336–340.

Cooper, R., Boninger, M., Kwarciak, A., and Ammer, B. (2002). Development of power wheelchair chin-operated force-sensing joystick. In *[Engineering in Medicine and Biology, 2002. 24th Annual Conference and the Annual Fall Meeting of the Biomedical Engineering Society] EMBS/BMES Conference, 2002. Proceedings of the Second Joint*, volume 3, pages 2373–2374. IEEE.

Elfes, A. (1989a). A tessellated probabilistic representation for spatial robot perception and navigation. *Proceedings NASA Publications*, 3(N90).

Elfes, A. (1989b). Using occupancy grids for mobile robot perception and navigation. *Computer*, 22(6):46–57.

Faria, B. M., Reis, L. P., and Lau, N. (2013). Manual, automatic and shared methods for controlling an intelligent wheelchair: Adaptation to cerebral palsy users. *In: 13th International Conference on Autonomous Robot Systems and Competitions*, pages 26–31.

Garrido, S., Moreno, L., Abderrahim, M., and Monar, F. M. (2006). Path planning for mobile robot navigation using voronoi diagram and fast marching. In *IROS*, pages 2376–2381. iSBN: 1-4244-0259-X.

Jeonghee, K., Xueliang, H., and Maysam, G. (2008). Wireless control of powered wheelchairs with tongue motion using tongue drive assistive technology. *Annual International Conference of the IEEE Engineering in Medicine and Biology Society. IEEE Engineering in Medicine and Biology Society. Conference*, 2008:4199–4202.

Jeonghee, K., Xueliang, H., Minocha, J., Holbrook, J., Laumann, A., and Maysam, G. (2012). Evaluation of a smartphone platform as a wireless interface between tongue drive system and electric-powered wheelchairs. *IEEE Trans. Biomed. Engineering*, 59(6):1787–1796.

Jiding, D., Zhijun, L., Chenguang, Y., and Peng, X. (2014). Shared control of a brain-actuated intelligent wheelchair. pages 341–346. IEEE.

Lund, M. E., Christiensen, H. V., Caltenco, H. A., Lontis, E. R., Bentsen, B., and Andreasen, S. L. N. (2010). Inductive tongue control of powered wheelchairs. In *Proceedings of the 32nd Annual International Conference of the IEEE Engineering in Medicine and Biology Society*, pages 3361–3364. Isbn = 978-1-4244-4123-5.

Moravec, H. and Elfes, A. (1985). High resolution maps from wide angle sonar. In *Robotics and Automation. Proceedings. 1985 IEEE International Conference on*, volume 2, pages 116–121. IEEE.

Petry, M., Paulo, A. M., Braga, R., and Paulo, L. R. (2010). Shared control for obstacle avoidance in intelligent wheelchairs. *in IEEE Conference on Robotics, Automation and Mechatronics*, pages 182–187.

Quigley, M., Conley, K., Gerkey, B., Faust, J., Foote, T. B., Leibs, J., Wheeler, R., and Ng, A. Y. (2009). ROS: an open-source robot operating system. In *ICRA Workshop on Open Source Software*.

San Agustin, J., Mateo, J., Paulin, H. J., and Villanueva, A. (2009). Evaluation of the potential of gaze input for game interaction. *PsychNology Journal*, 7(2):213–236.

Simpson, R. C., LoPresti, E. F., and Cooper, R. A. (2008). How many people would benefit from a smart wheelchair? *Journal of Rehabilitation Research and Development*, 45(1):53–72.

Stěpán, P., Kulic, M., and Přeučil, L. (2005). Robust data fusion with occupancy grids. In *IEEE Transactions on Systems, Man, and Cybernetics*, pages 106–115. IEEE.

Torsten, Felzer and Rainer, Nordman (2007). Alternative wheelchair control. In *Proc. Int. IEEE-BAIS Symp., Res. Assistive Technol.*, pages 67–74.

Xueliang, H. and Maysam, G. (2010). Evaluation of a wireless wearable tongue-computer interface by individuals with high-level spinal cord injuries. *Journal of Neural Engineering*, 7(2). ISBN: 17412560.